

Effective patient dose during neuroradiological C-arm CT procedures

Mei Bai, Xianghua Liu, Bin Liu

PURPOSE

We aimed to determine the effective dose given to patients during neuroradiological C-arm computed tomography (CT) procedures.

MATERIALS AND METHODS

Measurements were performed on 48 patients using a dose-area product (DAP) meter. A PC-based Monte Carlo program (PCXMC, STUK, Helsinki, Finland) was used to calculate the effective dose from the DAP values of each patient. Organ doses were also measured with thermoluminescent dosimeters (TLDs) using a human-shaped phantom.

RESULTS

The difference between the organ doses measured using TLDs and PCXMC was not significant ($P > 0.05$). The mean DAP for 48 patients was 9.41 ± 2.50 Gy·cm²; the mean effective dose for all procedures was 0.30 ± 0.08 mSv. The coefficient for the correlation (R^2) between the DAP and the effective dose was 0.97. The conversion factor between the effective dose and DAP was $0.030\text{--}0.035$ mSv·Gy⁻¹·cm⁻².

CONCLUSION

DAP can be used as a dose indicator to calculate the organ dose and effective dose of patients based on Monte Carlo simulation. This method can provide important information on the absorbed dose and enhance the radiation protection of patients during C-arm CT procedures.

C-arm flat panel computed tomography (CT) is new, innovative imaging technique that combines the C-arm design and three-dimensional (3D) cone-beam CT imaging, enabling both traditional angiographic imaging and soft tissue differentiation (1). C-arm flat panel angiographic systems use two-dimensional (2D) X-ray projection data acquired with a flat-panel detector to generate CT-like images (2–5). C-arm flat panel CT imaging has been used in a number of clinical applications (6–9). Neuroradiology also benefits from this 3D C-arm imaging system (10–13). Cerebral bleeding, bone imaging, and other high-contrast target imaging techniques are important C-arm CT applications in neuroradiology.

Like conventional X-ray imaging procedures, C-arm CT involves an additional radiation dose to the patient. Unlike a CT scanner, C-arm CT covers areas far larger than 100 mm (2). The CT dose index defined for standard CT might be adapted to this, but it is not yet standardized, and it is not the dose value displayed in the imaging unit (14).

Since C-arm CT was developed from angiography, many manufacturers provide the dose-area product (DAP), which is an important quantity for establishing a patient's stochastic risk, characterized by the effective dose. This study estimated the effective dose to patients undergoing neuroradiology procedures and derived the correlation between the effective dose and DAP. DAP values were collected for C-arm CT imaging. The effective dose was calculated using a PC-based Monte Carlo program.

Materials and methods

Patients

Forty-eight patients undergoing neuroradiology procedures (54.8 ± 9.5 years, 20 females) were examined using a DynaCT (AXIOM Artis dTA, Siemens Healthcare, Forchheim, Germany) C-arm CT. Automatic exposure control and a 5 s rotation time scan were used; 139 2D projections were acquired over the course of a 200° rotation of the X-ray tube around the patient. DAP values were collected using an air-ionization chamber DAP meter (Diamentor, PTW, Freiburg, Germany) incorporated in the housing of the under-the-couch tube. A correction factor for calibrating the chamber and electrometer was also applied (15).

Phantom

A male Anderson Radiation Therapy 200 phantom (ART-200, Fluke Biomedical, Cleveland, Ohio, USA) with embedded thermoluminescence dosimeters (TLDs) was used to assess the radiation exposure of the

From the Department of Biomedical Engineering (M.B. ✉ baimei12@yahoo.com, X.L., B.L.), Xuanwu Hospital of Capital Medical University, Beijing, China.

Received 9 April 2012; accepted 19 May 2012.

Published online 13 December 2012
DOI 10.4261/1305-3825.DIR.5852-12.0

C-arm CT and compared with the results of a Monte Carlo-based program (16). To calculate the effective dose according to ICRP 103 (17), TLDs were placed in 22 organ sites in the phantom according to the anatomical position of each "organ point", including the gonads, red bone marrow, colon, lung, stomach, bladder, breast, liver, esophagus, thyroid, skin, bone surface, brain, small intestine, kidney, pancreas, thymus, spleen, uterus, and salivary glands. Three TLDs were placed at each dose measurement point, and the organ dose was defined as the mean of the three TLDs. The TLDs were selected before use to keep the dispersion in $\pm 1\%$.

Dose calculation

A PC-based Monte Carlo program, (PCXMC, STUK, Helsinki, Finland) (18) was used to calculate the organ doses and effective dose for each of the 139 frames per patient separately and then the 139 effective doses were summed to give the global effective dose for the full C-arm CT run. Simulations were performed with patient-specific input parameters (weight and length) and the actual C-arm CT system settings for each projection, including the beam quality, X-ray tube characteristics, and dose level. The effective dose was calculated using the latest ICRP 103 weighing factors, published in 2007 (17).

Statistical analysis

Summary values are presented as means \pm standard deviation. Paired samples t tests were used to assess the differences between the measured organ doses using TLDs and the program PCXMC. All statistical tests were performed using a computer software (Statistical Package for Social Sciences, SPSS Inc., Chicago, Illinois, USA). A P value < 0.05 was deemed to indicate statistical significance.

Results

Radiation dose for phantom scan

The phantom (73.5 kg, 175 cm tall) was scanned under automatic exposure control and a 5 s rotation time

(70 kV, 216 mA, 139 projections). The total DAP was 10.30 Gy \cdot cm 2 . Under this condition, the effective dose from the TLD measurements was 0.33 mSv, while the effective dose from PCXMC was 0.28 mSv; the difference was not significant ($P = 0.502$).

Fig. 1a shows the effective dose to the patient for each projection calculated using PCXMC for the phantom scan. Fig. 1b plots some irradiated organ dose changes throughout a rotational run calculated using PCXMC for the phantom scan.

For the effective dose and organ dose, a clear dip is obvious in the middle frames; this is explained by the

automatic tube modulation leading to lower dose deposition in the tissues for those frames (19). The absorbed dose is especially high for the first and last few frames. The active bone marrow and skin doses had more homogeneous dose distributions because the organ doses are averaged over the total volume of the organ in the body. The averaged skin and active bone marrow doses were significantly lower than those to the other organs due to the small fraction of body skin exposed.

Radiation dose to patients

Fig. 2 shows the histogram of the DAP for 48 patients. The mean DAP was

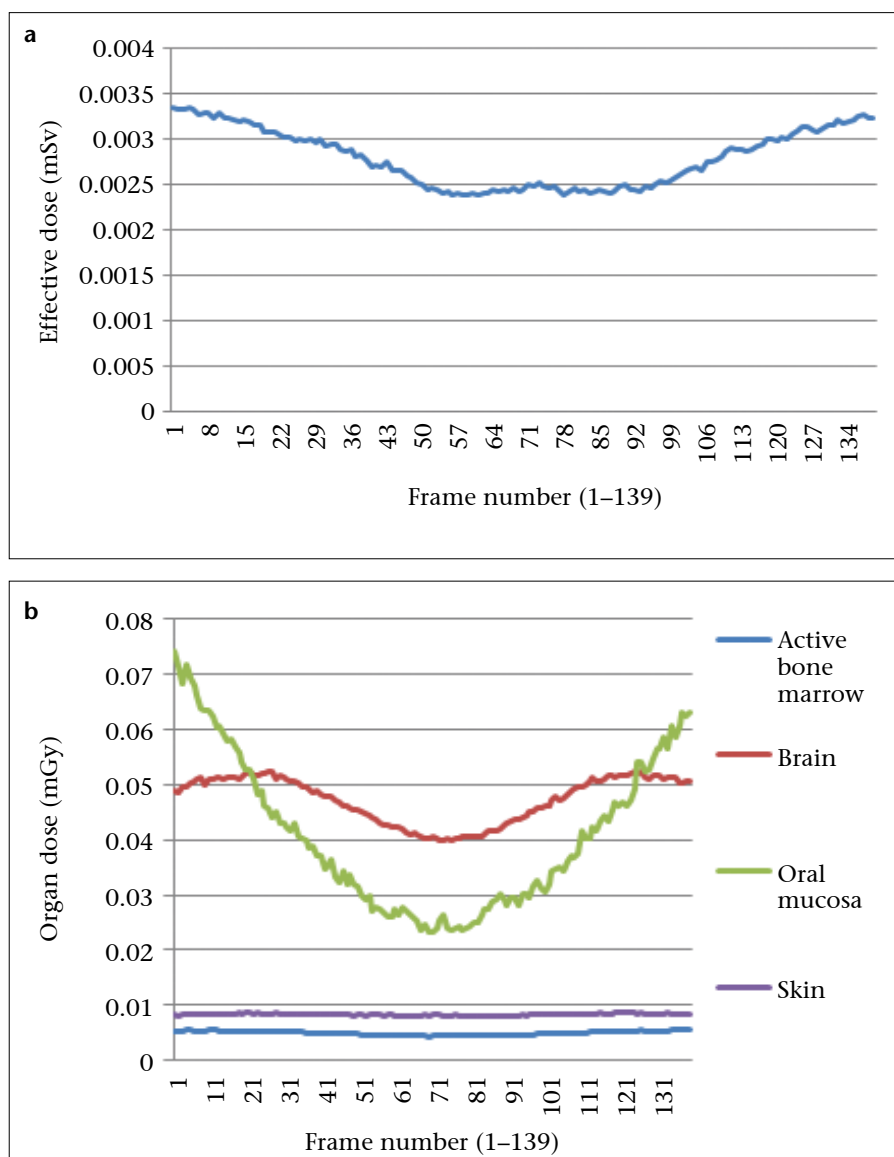


Figure 1. a, b. Effective dose (a) was calculated by a PC-based Monte Carlo program (PCXMC) for each of the 139 frames. Organ dose (b) was calculated by PCXMC for each individual frame.

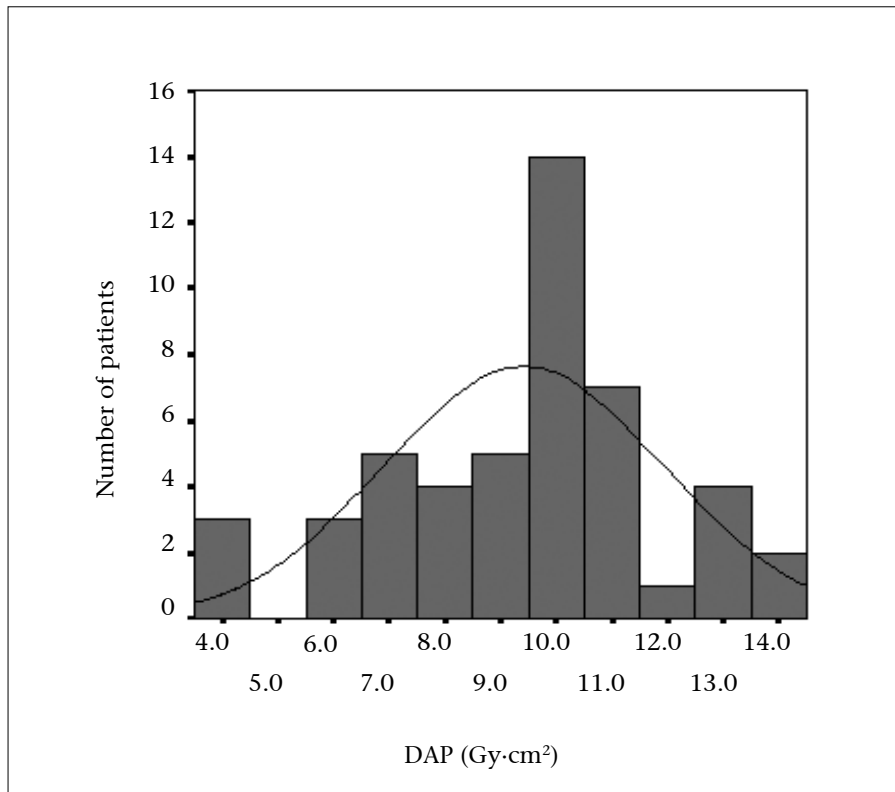


Figure 2. Histogram of dose-area product (DAP) (mean, 9.41 ± 2.50 Gy·cm²; n=48).

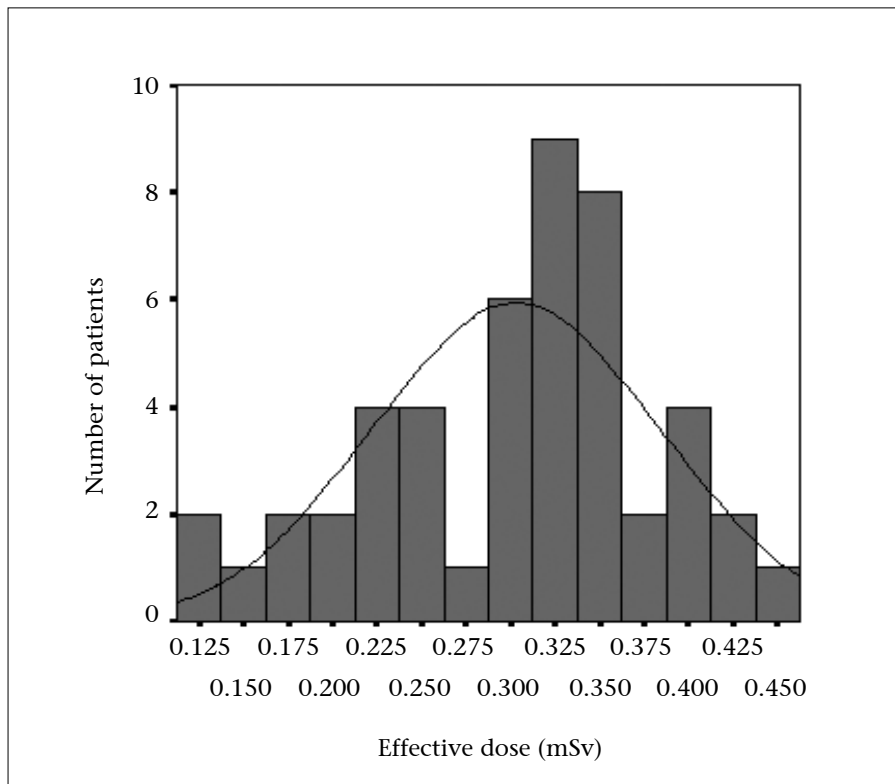


Figure 3. Histogram of effective dose (mean, 0.30 ± 0.08 mSv; n=48).

9.41 ± 2.50 Gy·cm² (range, 3.77–14.33 Gy·cm²). Fig. 3 shows the histogram of the effective dose for the 48 patients

calculated using PCXMC individually. The mean effective dose for all procedures was 0.30 ± 0.08 mSv (range 0.12–

0.43 mSv). Fig. 4 shows the correlation between DAP and the effective dose for the 48 patients. A linear effective dose increase with DAP was confirmed ($R^2=0.97$; $P < 0.05$). The conversion factor between the effective dose and DAP was 0.030–0.035 mSv·Gy⁻¹·cm⁻².

Discussion

Estimation of effective dose is a tough task in radiological imaging. Using TLD method to estimate the effective dose is very complicated and has bad operability in practical work. Therefore we introduced Monte Carlo simulations to the estimation of effective dose for C-arm CT. The present phantom study shows that the results of Monte Carlo simulations can be used for C-arm CT procedures. There was good agreement between the results of the calculation and TLD measurements ($P > 0.05$). The dose distribution in the direction of X-ray tube rotation was revealed using PCXMC. The distribution of the effective dose for each X-ray view shows that the dose curve dropped in the middle frames over C-arm CT; this indicates that the characteristics of the C-arm CT dose distribution differ from those of CT.

In conclusion, there was a good correlation ($R^2=0.97$) between the DAP and the effective dose per patient. Therefore, the total DAP per procedure gives a good indication of the radiation dose to the patient with C-arm CT. Consequently, the effective dose that characterizes a patient's stochastic risk can be estimated using easily measurable DAP values. We also believe that the use of an online measurement device such as a DAP meter that provides real-time information regarding the radiation dose is preferable to other methods, such as TLD measurement.

Acknowledgment

This work was supported by IAEA Research Contract No.16155/R0, the National Natural Sciences Foundation of China (NSFC) grant no. 30870751, and Beijing Municipal Health Bureau grant no. 2009-3-57.

Conflict of interest disclosure

The authors declared no conflicts of interest.

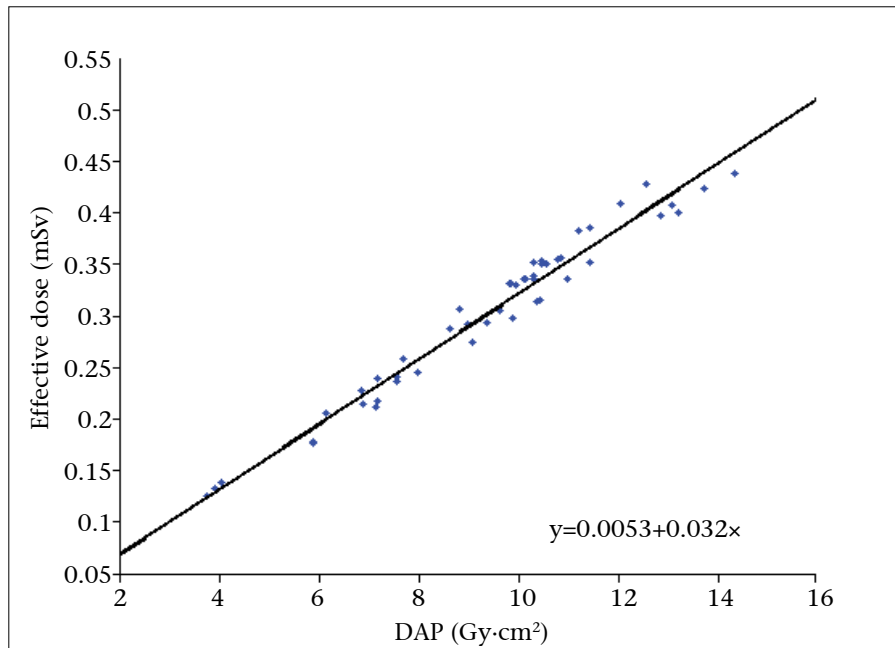


Figure 4. Correlation between dose-area product (DAP) and effective dose for each patient.

References

1. Kamran M, Nagaraja S, Byrne JV. C-arm flat detector computed tomography: the technique and its applications in interventional neuro-radiology. *Neuroradiology* 2010; 52:319–327. [CrossRef]
2. Reiser MF, Becker CR, Nikolaou K, Glazer G. Multislice CT: 3D imaging with flat-detector C-arm systems, 3rd ed. Berlin: Springer-Verlag, 2009; 34–49.
3. Jaffray DA, Siewerdsen JH. Cone-beam computed tomography with a flat-panel imager: initial performance characterization. *Med Phys* 2000; 27:1311–1323. [CrossRef]
4. Ritter D, Orman J, Schmidgunst C, Graumann R. 3D soft tissue imaging with a mobile C-arm. *Comput Med Imaging Graphics* 2007; 31:91–102. [CrossRef]
5. Kalender W, Kyriakou Y. Flat-detector computed tomography (FD-CT). *Eur Radiol* 2007; 17:2767–2779. [CrossRef]
6. Eide KR, Ødegård A, Myhre HO, Lydersen S, Hatlinghus S, Haraldseth O. DynaCT during EVAR—a comparison with multidetector CT. *Eur J Vasc Endovasc Surg* 2009; 37:23–30. [CrossRef]
7. Eide KR, Ødegård A, Myhre HO, Haraldseth O. Initial observations of endovascular aneurysm repair using Dyna-CT. *J Endovasc Ther* 2007; 14:50–53. [CrossRef]
8. Meyer BC, Frericks BB, Albrecht T, Wolf KJ, Wacker FK. Contrast-enhanced abdominal angiographic CT for intraabdominal tumor embolization: a new tool for vessel and soft-tissue visualization. *Cardiovasc Intervent Radiol* 2007; 30:743–749. [CrossRef]
9. Wallace MJ, Murthy R, Kamat PP, et al. Impact of C arm CT on hepatic arterial interventions for hepatic malignancies. *J Vasc Intervent Radiol* 2007; 18:1500–1507. [CrossRef]
10. Heran NS, Song JK, Namba K, Smith W, Niimi Y, Berenstein A. The utility of DynaCT in neuroendovascular procedures. *AJNR Am J Neuroradiol* 2006; 27:330–332.
11. Richter G, Engelhorn T, Struffert T, et al. Flat panel detector angiographic CT for stent-assisted coil embolization of broad-based cerebral aneurysms. *AJNR Am J Neuroradiol* 2007; 10:1902–1908. [CrossRef]
12. Engelhorn T, Rennert J, Richter G, Struffert T, Ganslandt O, Doerfler A. Myelography using flat panel volumetric computed tomography: a comparative study in patients with lumbar spinal stenosis. *Spine (Phila Pa 1976)* 2007; 32:E523–527.
13. Doelken M, Struffert T, Richter G, et al. Flat-panel detector volumetric CT for visualization of subarachnoid hemorrhage and ventricles: preliminary results compared to conventional CT. *Neuroradiology* 2008; 50:517–523. [CrossRef]
14. Kyriakou Y, Richter G, Dörfler A, Kalender WA. Neuroradiologic applications with routine C-arm flat panel detector CT: evaluation of patient dose measurements. *AJNR Am J Neuroradiol* 2010; 29:1930–1936. [CrossRef]
15. Larsson P, Alm Carlsson G, Persliden J, Sandborg M. Transmission ionization chambers for measurements of air collision kerma integrated over beam area: factors limiting the accuracy of calibration. *Phys Med Biol* 1996; 41:2381–2398. [CrossRef]
16. International Commission on Radiological Protection. ICRP Publication 23, Report of the Task Group on Reference Man. Oxford: Pergamon Press, 1975; 335–365.
17. International Commission on Radiological Protection. ICRP Publication 103, the 2007 Recommendation of the International Commission on Radiological Protection. Oxford: Elsevier Ltd., 2007; 60–318.
18. Servomaa A, Tapiovaara M. Organ dose calculation in medical X ray examinations by the program PCXMC. *Radiat Prot Dosimetry* 1998; 80:213–219. [CrossRef]
19. Wielandts JY, Buck SD, Ector J, et al. Three-dimensional cardiac rotational angiography: effective radiation dose and image quality implications. *Europace* 2010; 12:194–201. [CrossRef]